

Complex-Path Prediction of Resonance-Assisted Tunneling in Mixed Systems

Felix Fritzsche,^{1,2} Arnd Bäcker,^{1,2} Roland Ketzmerick,^{1,2} and Normann Mertig^{1,2,3}

¹Technische Universität Dresden, Institut für Theoretische Physik and Center for Dynamics, 01062 Dresden, Germany

²Max-Planck-Institut für Physik komplexer Systeme, Nöthnitzer Straße 38, 01187 Dresden, Germany

³Department of Physics, Tokyo Metropolitan University, Minami-Osawa, Hachioji 192-0397, Japan

(Dated: June 16, 2022)

We present a semiclassical prediction of regular-to-chaotic tunneling in systems with a mixed phase space, including the effect of a nonlinear resonance chain. We identify complex paths for direct and resonance-assisted tunneling in the phase space of an integrable approximation with one nonlinear resonance chain. We evaluate the resonance-assisted contribution analytically and give a prediction based on just a few properties of the classical phase space. For the standard map excellent agreement with numerically determined tunneling rates is observed.

In typical Hamiltonian systems regions of regular and chaotic motion coexist in a mixed phase space. Although, both types of motion are strictly separated in classical mechanics they are connected in quantum mechanics due to dynamical tunneling [1, 2]. This effect is crucial for a rich variety of systems. For example dynamical tunneling influences the vibrational spectrum of molecules [1], determines ionization rates of atoms in laser fields [3, 4], and describes chaos-assisted tunneling oscillations [5, 6] of cold atom systems [7, 8]. In optics dynamical tunneling is experimentally explored in microwave resonators [9–12] as well as moderately deformed microlasers [13–20], where it determines the quality factor of lasing modes. Recently, the enhancement of dynamical tunneling by resonance-assisted tunneling [21, 22] was demonstrated experimentally [12, 17].

To reveal the universal features of dynamical tunneling in systems with a mixed phase space it is extensively studied theoretically [10, 13, 23–43], mainly in model systems. A central object is the tunneling rate γ_m , which describes the transition from a state on the m th quantizing torus of the regular region into the chaotic sea. A qualitative understanding of γ_m can be obtained from resonance-assisted tunneling [21, 22, 27, 44], see dashed line in Fig. 1(b). On average it predicts an exponential decay of γ_m with the inverse effective Planck constant h . However, for some values of h a drastic enhancement of γ_m is observed, due to the coupling of regular states. This is induced by a nonlinear resonance chain which generically occurs inside the regular region of non-integrable systems [45], see Fig. 1(a).

A more accurate prediction of tunneling rates is obtained when combining the perturbation theory of resonance-assisted tunneling with direct tunneling predictions [31, 38]. Recently a non-perturbative prediction of resonance-assisted tunneling was achieved [43]. These methods are based on integrable approximations of the regular region [46, 47], whose construction requires some numerical effort. However, an intuitive semiclassical picture of these tunneling phenomena in terms of classical trajectories is still lacking. Such semiclassical theories exist only for time-domain quantities [23, 24], direct tun-

neling rates for cases when resonances are irrelevant [39], and integrable systems [48].

In this paper we present a semiclassical formula of resonance-assisted regular-to-chaotic tunneling rates. It can be approximated leading to a semiclassical formula requiring just a few properties of the classical mixed phase space. Excellent agreement with numerical results for the standard map is observed, see Fig. 1(b).

Overview — We obtain the semiclassical prediction based on an integrable approximation including one non-

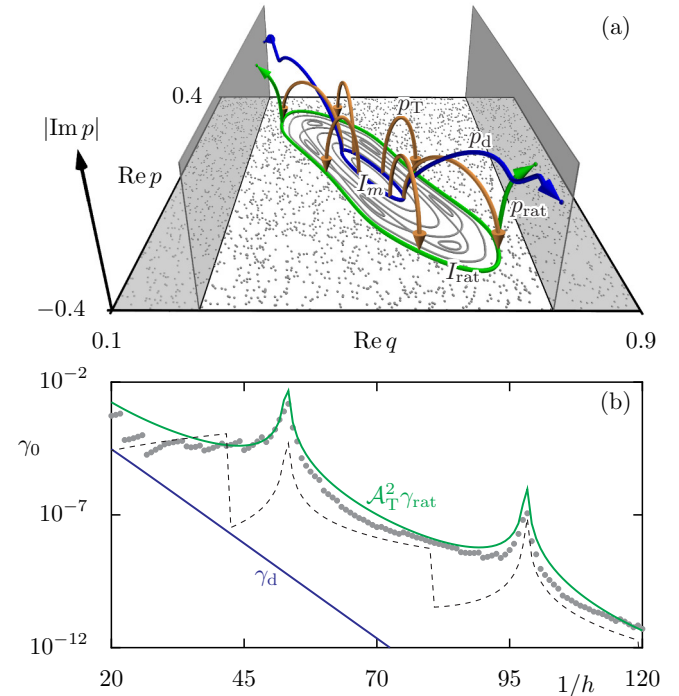


FIG. 1. (a) Phase space of the standard map for $\kappa = 3.4$ with regular tori (thin [gray] lines), chaotic orbits ([gray] dots) and the leaky region (shaded areas). The real tori and complex paths are labeled in the figure and described in the text. (b) Tunneling rate γ_0 vs. $1/h$. Numerically obtained rates (dots) are compared with γ_d and an analytic evaluation of $A_T^2 \gamma_{\text{rat}}$. The perturbative result [44] is shown as dashed line.

linear resonance chain [47]. This allows for extending semiclassical methods from integrable [48] to mixed systems. Within the integrable approximation we perform a WKB analysis of real tori and complex tunneling paths connecting the regular region with the chaotic sea. This gives the tunneling rate

$$\gamma_m = \gamma_d + \mathcal{A}_T^2 \gamma_{\text{rat}}, \quad (1)$$

which is composed of a direct contribution γ_d and a resonance-assisted contribution $\mathcal{A}_T^2 \gamma_{\text{rat}}$, see (blue and green) lines in Fig. 1(b). Figure 1(a) gives an illustration of the phase-space structures contributing to Eq. (1):

(i) Quantizing torus I_m and direct tunneling paths p_d : The quantizing torus I_m , associated with the m th regular state, gives rise to tunneling paths $p_d(q)$ with complex momentum emanating from the turning points of I_m . See (blue) inner ring and arrows, respectively. They connect I_m with the chaotic sea and determine the direct tunneling rate γ_d , Eq. (7).

(ii) Partner torus I_{rat} and resonance-assisted tunneling paths p_{rat} : A partner torus with action I_{rat} on the opposite side of the nonlinear resonance is connected with the chaotic sea by complex tunneling paths $p_{\text{rat}}(q)$, see (green) outer ring and arrows. They lead to the resonance-assisted tunneling rate γ_{rat} , Eq. (7).

(iii) Tunneling paths p_T : The tori I_m and I_{rat} are connected by complex paths $p_T(q)$ bridging the resonance, see (orange) arrows. They determine the tunneling amplitude \mathcal{A}_T , Eq. (6).

Basic setting — We derive our results for kicked one-dimensional Hamiltonians $H(q, p, t) = T(p) + V(q) \sum_n \delta(t - n)$. For illustrations we use $T(p) = p^2/2$ and $V(q) = \kappa \cos(2\pi q)/(4\pi^2)$, giving the paradigmatic standard map [49], which is widely used to study tunneling phenomena [27, 31, 38, 43, 44]. At $\kappa = 3.4$ the corresponding stroboscopic Poincaré map exhibits a mixed phase space as shown in Fig. 1(a) with regions of regular motion (thin [gray] lines) and chaotic motion (dots). It is governed by a regular island containing a prominent $r:s=6:2$ nonlinear resonance chain and a surrounding chaotic sea. Quantum mechanically the dynamics is given by the unitary time-evolution operator $\hat{U} = \exp(-iV(\hat{q})/\hbar) \exp(-iT(\hat{p})/\hbar)$. By introducing a leaky region \mathcal{L} (shaded areas in Fig. 1(a)) close to the regular-chaotic border we compute tunneling rates γ_m as discussed in Ref. [43]. We focus on the ground state $m = 0$ living on the innermost quantizing torus within the regular island, whose tunneling rate is shown in Fig. 1(b) (dots). Note that higher excited states $m > 0$ show qualitatively the same features as γ_0 .

Integrable approximation — The key tool for deriving our prediction is an integrable approximation. It is a one degree of freedom time-independent Hamiltonian, which resembles the regular dynamics of the original system [47]. It is based on the universal description of the classical dynamics in the vicinity of a $r:s$ resonance by the

pendulum Hamiltonian [21, 22, 47, 50]

$$\mathcal{H}_{r:s}(\theta, I) = \mathcal{H}_0(I) + 2V_{r:s} \left(\frac{I}{I_{r:s}} \right)^{r/2} \cos(r\theta), \quad (2)$$

using action-angle coordinates of $\mathcal{H}_0(I)$. It is determined by the frequencies $\omega_0(I)$ of tori in the co-rotating frame of the resonance, as $\omega_0(I) = \partial_I \mathcal{H}_0(I)$ [47], where $\mathcal{H}_0(I) \approx (I - I_{r:s})^2/(2M_{r:s})$ close to the resonant torus $I_{r:s}$. The quantities $I_{r:s}$, $V_{r:s}$, and $M_{r:s}$ can be computed from the position and the size of the resonance chain and the linearized dynamics of its central orbit [27, 47]. The phase space is depicted by thin [gray] lines in Fig. 2. Via a canonical transformation T the Hamiltonian Eq. (2) is mapped onto the phase space of the standard map giving $H_{r:s}(q, p) = \mathcal{H}_{r:s}(T^{-1}(q, p))$ [47]. By quantizing and diagonalizing $H_{r:s}$ its eigenstates ψ_m yield the tunneling rate [43]

$$\gamma_m = \int_{\mathcal{L}} |\psi_m(q)|^2 dq, \quad (3)$$

via the probability of $\psi_m(q)$ on the leaky region \mathcal{L} , which we evaluate semiclassically in the following.

WKB construction — Using WKB-techniques [51, 52] we now construct the state ψ_m within the integrable approximation $H_{r:s}(q, p)$. This extends the semiclassical methods developed for integrable systems [48] to systems with a mixed phase space. Furthermore, the use of the integrable approximation overcomes the problem of natural boundaries [53, 54].

Following [52], the WKB-construction of the wave function $\psi_m(q)$ within the integrable approximation requires the solutions $p_\alpha(q)$ of the equation $E_m = H_{r:s}(q, p_\alpha(q))$, as depicted in Fig. 1(a). Here, E_m is the energy of the wave function $\psi_m(q)$ and the position coordinate q is real. The real solutions $p_\alpha(q)$ describe the wave function in classically allowed regions. The complex solutions $p_\alpha(q)$ describe the tunneling tails of the wave function in classically forbidden regions. In particular, they describe $\psi_m(q)$ in the leaky region, as required by Eq. (3).

Specifically, for resonances the geometry of paths gives the semiclassical wave function as a superposition

$$\psi_m(q) = \psi_d(q) + \mathcal{A}_T \psi_{\text{rat}}(q). \quad (4)$$

Here, (i) $\psi_d(q)$ is the direct wave function, (ii) $\psi_{\text{rat}}(q)$ is the resonant wave function, and (iii) \mathcal{A}_T is the tunneling amplitude. We now explain this in more detail:

(i) $\psi_d(q)$ describes the wave function along the quantizing torus $I_m = \hbar(m + 1/2)$ in the classically allowed region of energy $E_m \approx \mathcal{H}_0(I_m)$. Using Airy-type connections [52] this wave function is extended into the classically forbidden region along the paths $(q, p_\alpha(q))$ (with $\alpha = d$), see Fig. 1(a), as

$$\psi_\alpha(q) = \left| \frac{\omega_0(I_m)}{2\pi \partial_p H_{r:s}(q, p_\alpha(q))} \right|^{1/2} \exp \left(\frac{i}{\hbar} \int p_\alpha(\tilde{q}) d\tilde{q} \right). \quad (5)$$

Here, $\omega_0(I_m)/(2\pi)$ accounts for global normalization of the wave function, while $1/|\partial_p H_{r:s}(q, p_\alpha(q))|$ is the classical probability along $p_\alpha(q)$. The complex action $\int p_\alpha(q) dq$, for which the lower limit is one of the turning points on the torus I_m , describes direct tunneling into the leaky region.

(ii) Due to the presence of the nonlinear resonance there is an additional real solution I_{rat} with energy E_m on the opposite side of the resonance chain. Along this torus I_{rat} we construct the wave function $\psi_{\text{rat}}(q)$. In particular, the tunneling tails associated with the solutions $p_{\text{rat}}(q)$ emanating from I_{rat} and connecting to the chaotic part of phase space, see Fig. 1(a), also obey Eq. (5) with $\alpha = \text{rat}$. Note that $\omega_0(I_m)/(2\pi)$ in Eq. (5) must be kept for normalization. The lower limit of the action integral is one of the turning points on I_{rat} .

(iii) Finally, the tunneling amplitude is given by [22]

$$\mathcal{A}_T = \left| 2 \sin \left(\frac{\pi}{r\hbar} [I_{\text{rat}} - I_m] \right) \right|^{-1} \exp \left(-\frac{\sigma}{\hbar} \right), \quad (6)$$

where $\sigma = \text{Im} \int p_T(q) dq$ is the imaginary part of the action of any path $p_T(q)$ connecting I_m to I_{rat} . In particular, since there is no solution $p_\alpha(q)$ connecting I_m and I_{rat} along real positions, these paths are only sketched schematically in Fig. 1(a). Note that this evaluation of \mathcal{A}_T based on paths with complex position is formally beyond the WKB-construction used here. It has been introduced and successfully applied for near-integrable systems in Ref. [48]. Further note that complex solutions which do not connect to a real torus are neglected.

To summarize our construction, the wave functions $\psi_d(q)$ and $\psi_{\text{rat}}(q)$, Eq. (5), together with the tunneling amplitude, Eq. (6), give the wave function $\psi_m(q)$, Eq. (4). Inserting $\psi_m(q)$ into Eq. (3) and neglecting interference allows for evaluating the integral in Eq. (3) independently for $\psi_d(q)$ and $\psi_{\text{rat}}(q)$. For solving these integrals we linearize the action integral in Eq. (5) around the boundary of the leaky region at $q_{\mathcal{L}}$. We further account for the symmetry of the standard map with respect to the central fixed point. This gives (i) the direct ($\alpha = d$) and (ii) the resonance-assisted ($\alpha = \text{rat}$) tunneling rate as

$$\gamma_\alpha = \frac{\hbar}{\text{Im} p_\alpha(q_{\mathcal{L}})} |\psi_\alpha(q_{\mathcal{L}})|^2, \quad (7)$$

i. e., each tunneling rate is given by the value of the normalized WKB wave function at the boundary $q_{\mathcal{L}}$ of the leaky region.

This construction constitutes our first main result. Numerical evaluation of the semiclassically obtained tunneling rates shows excellent agreement with numerical obtained tunneling rates (not shown). It further reveals that for the standard map at $\kappa = 3.4$ the resonance-assisted contribution dominates the semiclassically predicted decay rates for all values of the effective Planck constant. In general, one should have $\gamma_m = \mathcal{A}_T^2 \gamma_{\text{rat}}$,

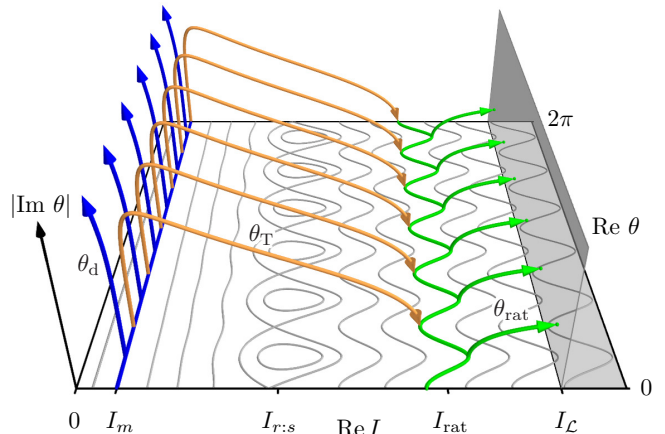


FIG. 2. Phase space of $\mathcal{H}_{r:s}$ (thin [gray] lines) and leaky region \mathcal{L} (shaded area). Real tori and complex paths (thick lines and arrows) are labeled in the figure.

whenever the resonance is sufficiently large, roughly speaking when it is visible within the regular region. The converse, that is γ_m being dominated by the direct tunneling rate γ_d may occur for small values of $1/\hbar$ or if the resonance is extremely small.

Approximation of $\mathcal{A}_T^2 \gamma_{\text{rat}}$ — In the following we derive an analytic formula which evaluates the dominating term $\mathcal{A}_T^2 \gamma_{\text{rat}}$ based on just a few properties of the classical phase space. To this end we use the pendulum Hamiltonian $\mathcal{H}_{r:s}(\theta, I)$, Eq. (2), in action-angle coordinates of $\mathcal{H}_0(I)$ and the action representation $\psi_m(I)$ of the WKB wave function, respectively. This extends the WKB construction presented in Ref. [22] to the Hamiltonian (2).

As a first approximation we extend the leaky region to all chaotic trajectories, as $I > I_{\mathcal{L}}$ (shaded area in Fig. 2). In order to account for sticky motion, we choose $I_{\mathcal{L}}$ such that $2\pi I_{\mathcal{L}}$ is the area enclosing the regular region enlarged up to the most relevant partial barrier [27, 44]. While the basic features of γ_m are preserved upon changing the leaky region, it is worth noting that its details might change roughly up to two orders of magnitude [43]. This constitutes the main error of our prediction.

To construct the WKB wave function the classical phase-space structures $\theta_\alpha(I)$ fulfilling $\mathcal{H}_{r:s}(\theta, I) = E_m$ for real actions are required. They are depicted in Fig. 2 and obey $\cos(r\theta) = \varphi(I)$, where

$$\varphi(I) = \left(\frac{I_{r:s}}{I} \right)^{r/2} \frac{E_m - \mathcal{H}_0(I)}{2V_{r:s}}. \quad (8)$$

Real solutions correspond to the tori oscillating around I_m and I_{rat} , i.e. the classically allowed regions ([blue and green] thick lines) on opposite sides of the resonance chain at $I_{r:s}$. We have $I_m = \hbar(m+1/2)$ and a reasonable approximation of I_{rat} is obtained from $I_{\text{rat}} \approx 2I_{r:s} -$

$I_m + [E_m - \mathcal{H}_0(2I_{r:s} - I_m)]/\omega_0(2I_{r:s} - I_m)$. The torus I_m is accompanied by complex paths $\theta_d(I)$ ([blue] arrows) which emanate from turning points with $I < I_m$ and diverge at $I = 0$. Furthermore, there are tunneling paths $\theta_T(I)$ ([orange] arrows) with imaginary part $\text{Im } \theta_T(I) = \text{arccosh}(|\varphi(I)|)/r$ attached to turning points with $I > I_m$ bridging the resonance towards I_{rat} . Finally, there are complex paths $\theta_{\text{rat}}(I)$ ([green] arrows) emanating from turning points with $I > I_{\text{rat}}$ on the partner torus. They have imaginary part $\text{Im } \theta_{\text{rat}}(I) = \text{arccosh}(|\varphi(I)|)/r$ as well and connect I_{rat} with the leaky region.

Using Eq. (5), with accordingly interchanged phase-space coordinates, local WKB wave functions can be constructed from these paths. Again a global construction of $\psi_m(I)$ is obtained by using Airy-type connections at classical turning points [22, 52]. In action-angle coordinates the torus I_m is not directly connected with the leaky region. Thus, for $\psi_m(I)$ there is neither a direct contribution to the WKB wave function within \mathcal{L} nor a direct tunneling rate γ_d involved in this construction. Consequently, one has $\psi_m(I) = \mathcal{A}_T \psi_{\text{rat}}(I)$ within \mathcal{L} . As the tunneling amplitude \mathcal{A}_T , Eq. (6), is canonically invariant, it can be computed in action-angle coordinates as well, requiring the evaluation of $\sigma = \text{Im} \int \theta_T dI$ from I_m to I_{rat} . By approximating $\text{Im } \theta_T(I) \approx \ln(2|\varphi(I)|)/r$, which is justified if $V_{r:s} \ll E_m$, and using only the quadratic part of $\mathcal{H}_0(I)$, we find

$$\begin{aligned} \sigma &= \frac{I_{\text{rat}} - I_m}{r} \ln \left(\frac{(I_{\text{rat}} - I_m)^2}{2e^2 M_{r:s} V_{r:s}} \right) \\ &+ \frac{I_m}{2} \ln \left(\frac{I_m}{eI_{r:s}} \right) - \frac{I_{\text{rat}}}{2} \ln \left(\frac{I_{\text{rat}}}{eI_{r:s}} \right), \end{aligned} \quad (9)$$

which inserted in Eq. (6) constitutes the first part of our analytic expression. Note that the first term coincides with the results obtained for a simpler pendulum model in Ref. [22] while the remaining terms are related to the action dependence of the resonance term proportional to $V_{r:s}$ in Eq. (2).

We proceed by computing γ_{rat} by Eq. (3) from the WKB wave function $\psi_{\text{rat}}(I)$ and its probability inside the leaky region. The WKB wave function $\psi_{\text{rat}}(I)$ is associated with $\theta_{\text{rat}}(I)$ and computed analogously to Eq. (5) using action-angle coordinates. Linearizing the tunneling action occurring in the exponential in Eq. (5) around $I_{\mathcal{L}}$ then gives

$$\gamma_{\text{rat}} = \frac{r\hbar}{2 \ln(2|\varphi(I_{\mathcal{L}})|)} |\psi_{\text{rat}}(I_{\mathcal{L}})|^2, \quad (10)$$

which is in close analogy with Eq. (7). Again the resonance-assisted tunneling rate is determined by the normalized WKB wave function

$$|\psi_{\text{rat}}(I_{\mathcal{L}})|^2 = \left| \frac{\omega_0(I_m)}{2r\pi(E_m - \mathcal{H}_0(I_{\mathcal{L}}))} \right| \exp \left(-\frac{2}{\hbar} \mathcal{S}_{\text{rat}} \right) \quad (11)$$

at the boundary of the leaky region. The tunneling action $\mathcal{S}_{\text{rat}} = \text{Im} \int \theta_{\text{rat}} dI$ from I_{rat} to $I_{\mathcal{L}}$ is evaluated similarly as Eq. (9) leading to

$$\begin{aligned} \mathcal{S}_{\text{rat}} &= \frac{I_{\mathcal{L}} - I_{\text{rat}}}{r} \ln \left(\frac{(I_{\mathcal{L}} - I_{\text{rat}})(I_{\mathcal{L}} - I_m)}{2e^2 M_{r:s} V_{r:s}} \right) \\ &+ \frac{I_{\text{rat}}}{2} \ln \left(\frac{I_{\text{rat}}}{eI_{r:s}} \right) - \frac{I_{\mathcal{L}}}{2} \ln \left(\frac{I_{\mathcal{L}}}{eI_{r:s}} \right) \\ &+ \frac{I_{\text{rat}} - I_m}{r} \ln \left(\frac{I_{\mathcal{L}} - I_m}{I_{\text{rat}} - I_m} \right), \end{aligned} \quad (12)$$

which concludes the computation of γ_{rat} .

Discussion — The evaluation of $\mathcal{A}_T^2 \gamma_{\text{rat}}$, based on the analytic expressions in Eqs. (9)–(12), requires just a few classical quantities, namely $I_{r:s}$, $V_{r:s}$, and $M_{r:s}$ as well as the frequencies $\omega_0(I)$. This analytic prediction is in excellent agreement with numerically obtained rates, see Fig. 1(b). The resonance peaks originate from the divergence of the prefactor \mathcal{A}_T , Eq. (6), i. e., they appear whenever I_{rat} fulfills a quantization condition $I_{\text{rat}} = \hbar(m + lr + 1/2)$. In particular, at the resonance peak a hybridization between states associated with the m th and $(m + lr)$ th quantizing torus occurs. This is the same resonance condition as obtained from perturbation theory [21]. In contrast, away from the resonance peak the tori I_m and I_{rat} are still energetically degenerate. However, since I_{rat} does not fulfill a quantization condition there is no associated quantum state. This is different from the perturbative framework, where several quantizing tori of different energy contribute to the final prediction. Finally, in contrast to perturbation theory, our result is dominated by a single term for all values of the effective Planck constant. Its overall exponential decay is dominated by the first term of the action σ , Eq. (9). Hence, the slope of the exponential decay, as depicted in Fig 1(b), is roughly proportional to the width of the dynamical tunneling barrier $I_{\text{rat}} - I_m$. Furthermore, it logarithmically depends on the ratio of (a) the area enclosed by the the resonant torus, proportional to $2I_{r:s} \approx (I_{\text{rat}} - I_m)$ and (b) the separatrix area of the resonance chain, which is proportional to $\sqrt{M_{r:s} V_{r:s}}$.

Summary and outlook — In conclusion we have derived a semiclassical prediction of resonance-assisted regular-to-chaotic tunneling rates in systems with a mixed phase space based on integrable approximations including one nonlinear resonance. We identified complex paths for (i) direct and (ii) resonance-assisted tunneling, from which the latter dominates the tunneling rates for all values of the effective Planck constant. This covers the experimentally accessible regime of large tunneling rates when only a single resonance is relevant. Furthermore, a closed analytic expression for the resonance-assisted contribution to the tunneling rates was derived. Testing our theory with the paradigmatic example of the standard map we find excellent agreement with numerically determined tunneling rates. As our expression solely

depends on just a few properties of the classical phase space it allows for a straightforward application to other systems with similar phase-space structures. In particular, quality factors of lasing modes in optical cavities or ionization rates of atoms in laser fields should be computable by means of the methods introduced in this paper.

We gratefully acknowledge fruitful discussions with Yasutaka Hanada, Kensuke Ikeda, Julius Kullig, Clemens Löbner, Steffen Löck, Amaury Mouchet, Peter Schlagheck, and Akira Shudo. We acknowledge support by the Deutsche Forschungsgemeinschaft (DFG) Grant No. BA 1973/4-1. N.M. acknowledges successive support by JSPS (Japan) Grant No. PE 14701 and Deutsche Forschungsgemeinschaft (DFG) Grant No. ME 4587/1-1.

-
- [1] M. J. Davis and E. J. Heller, Quantum dynamical tunneling in bound states, *J. Chem. Phys.* **75**, 246 (1981).
- [2] S. Keshavamurthy and P. Schlagheck, *Dynamical Tunneling: Theory and Experiment*, Taylor & Francis, Boca Raton (2011).
- [3] S. Wimberger, P. Schlagheck, C. Eltschka, and A. Buchleitner, Resonance-assisted decay of nondispersive wave packets, *Phys. Rev. Lett.* **97**, 043001 (2006).
- [4] J. Zakrzewski, D. Delande, and A. Buchleitner, Ionization via chaos assisted tunneling, *Phys. Rev. E* **57**, 1458 (1998).
- [5] W. A. Lin and L. E. Ballentine, Quantum tunneling and chaos in a driven anharmonic oscillator, *Phys. Rev. Lett.* **65**, 2927 (1990).
- [6] O. Bohigas, S. Tomsovic, and D. Ullmo, Manifestations of classical phase space structures in quantum mechanics, *Phys. Rep.* **223**, 43 (1993).
- [7] W. K. Hensinger et al., Dynamical tunnelling of ultracold atoms, *Nature* **412**, 52 (2001).
- [8] D. A. Steck, W. H. Oskay, and M. G. Raizen, Observation of chaos-assisted tunneling between islands of stability, *Science* **293**, 274 (2001).
- [9] C. Dembowski, H.-D. Gräf, A. Heine, R. Hofferbert, H. Rehfeld, and A. Richter, First experimental evidence for chaos-assisted tunneling in a microwave annular billiard, *Phys. Rev. Lett.* **84**, 867 (2000).
- [10] A. Bäcker, R. Ketzmerick, S. Löck, M. Robnik, G. Vidmar, R. Höhmann, U. Kuhl, and H.-J. Stöckmann, Dynamical tunneling in mushroom billiards, *Phys. Rev. Lett.* **100**, 174103 (2008).
- [11] B. Dietz, T. Guhr, B. Gutkin, M. Miski-Oglu, and A. Richter, Spectral properties and dynamical tunneling in constant-width billiards, *Phys. Rev. E* **90**, 022903 (2014).
- [12] S. Gehler, S. Löck, S. Shinohara, A. Bäcker, R. Ketzmerick, U. Kuhl, and H.-J. Stöckmann, Experimental observation of resonance-assisted tunneling, *Phys. Rev. Lett.* **115**, 104101 (2015).
- [13] V. A. Podolskiy and E. E. Narimanov, Chaos-assisted tunneling in dielectric microcavities, *Opt. Lett.* **30**, 474 (2005).
- [14] S. Shinohara, T. Harayama, T. Fukushima, M. Hentschel, T. Sasaki, and E. E. Narimanov, Chaos-assisted directional light emission from microcavity lasers, *Phys. Rev. Lett.* **104**, 163902 (2010).
- [15] S. Shinohara, T. Harayama, T. Fukushima, M. Hentschel, S. Sunada, and E. E. Narimanov, Chaos-assisted emission from asymmetric resonant cavity microlasers, *Phys. Rev. A* **83**, 053837 (2011).
- [16] J. Yang, S.-B. Lee, S. Moon, S.-Y. Lee, S. W. Kim, T. T. A. Dao, J.-H. Lee, and K. An, Pump-induced dynamical tunneling in a deformed microcavity laser, *Phys. Rev. Lett.* **104**, 243601 (2010).
- [17] H. Kwak, Y. Shin, S. Moon, S.-B. Lee, J. Yang, and K. An, Nonlinear resonance-assisted tunneling induced by microcavity deformation, *Scientific Reports* **5**, 9010 (2015).
- [18] H. Cao and J. Wiersig, Dielectric microcavities: Model systems for wave chaos and non-hermitian physics, *Rev. Mod. Phys.* **87**, 61 (2015).
- [19] C.-H. Yi, H.-H. Yu, J.-W. Lee, and C.-M. Kim, Fermi resonance in optical microcavities, *Phys. Rev. E* **91**, 042903 (2015).
- [20] C.-H. Yi, H.-H. Yu, and C.-M. Kim, Resonant torus-assisted tunneling, *Phys. Rev. E* **93**, 012201 (2016).
- [21] O. Brodier, P. Schlagheck, and D. Ullmo, Resonance-assisted tunneling in near-integrable systems, *Phys. Rev. Lett.* **87**, 064101 (2001).
- [22] O. Brodier, P. Schlagheck, and D. Ullmo, Resonance-assisted tunneling, *Ann. Phys. (N.Y.)* **300**, 88 (2002).
- [23] A. Shudo and K. S. Ikeda, Complex classical trajectories and chaotic tunneling, *Phys. Rev. Lett.* **74**, 682 (1995).
- [24] A. Shudo and K. S. Ikeda, Chaotic tunneling: A remarkable manifestation of complex classical dynamics in non-integrable quantum phenomena, *Physica D* **115**, 234 (1998).
- [25] V. A. Podolskiy and E. E. Narimanov, Semiclassical description of chaos-assisted tunneling, *Phys. Rev. Lett.* **91**, 263601 (2003).
- [26] S. Keshavamurthy, Dynamical tunneling in molecules: role of the classical resonances and chaos, *J. Chem. Phys.* **119**, 161 (2003).
- [27] C. Eltschka and P. Schlagheck, Resonance- and chaos-assisted tunneling in mixed regular-chaotic systems, *Phys. Rev. Lett.* **94**, 014101 (2005).
- [28] S. Keshavamurthy, On dynamical tunneling and classical resonances, *J. Chem. Phys.* **122**, 114109 (2005).
- [29] M. Sheinman, S. Fishman, I. Guarneri, and L. Rebuzzini, Decay of quantum accelerator modes, *Phys. Rev. A* **73**, 052110 (2006).
- [30] S. Keshavamurthy, Dynamical tunneling in molecules: quantum routes to energy flow, *Int. Rev. Phys. Chem.* **26**, 521 (2007).
- [31] A. Bäcker, R. Ketzmerick, S. Löck, and L. Schilling, Regular-to-chaotic tunneling rates using a fictitious integrable system, *Phys. Rev. Lett.* **100**, 104101 (2008).
- [32] A. Shudo and K. S. Ikeda, Stokes geometry for the quantum Hénon map, *Nonlinearity* **21**, 1831 (2008), 00001.
- [33] A. Shudo, Y. Ishii, and K. S. Ikeda, Chaos attracts tunneling trajectories: A universal mechanism of chaotic tunneling, *Europhys. Lett.* **81**, 50003 (2008), 00013.
- [34] A. Shudo, Y. Ishii, and K. S. Ikeda, Julia sets and chaotic tunneling: I, *J. Phys. A* **42**, 265101 (2009).
- [35] A. Shudo, Y. Ishii, and K. S. Ikeda, Julia sets and chaotic tunneling: II, *J. Phys. A* **42**, 265102 (2009).

- [36] A. Bäcker, R. Ketzmerick, S. Löck, J. Wiersig, and M. Hentschel, Quality factors and dynamical tunneling in annular microcavities, *Phys. Rev. A* **79**, 063804 (2009).
- [37] A. Bäcker, R. Ketzmerick, and S. Löck, Direct regular-to-chaotic tunneling rates using the fictitious-integrable-system approach, *Phys. Rev. E* **82**, 056208 (2010).
- [38] S. Löck, A. Bäcker, R. Ketzmerick, and P. Schlagheck, Regular-to-chaotic tunneling rates: From the quantum to the semiclassical regime, *Phys. Rev. Lett.* **104**, 114101 (2010).
- [39] N. Mertig, S. Löck, A. Bäcker, R. Ketzmerick, and A. Shudo, Complex paths for regular-to-chaotic tunnelling rates, *Europhys. Lett.* **102**, 10005 (2013).
- [40] Y. Hanada, A. Shudo, and K. S. Ikeda, Origin of the enhancement of tunneling probability in the nearly integrable system, *Phys. Rev. E* **91**, 042913 (2015).
- [41] A. Shudo and K. S. Ikeda, Toward pruning theory of the Stokes geometry for the quantum Hénon map, *Nonlinearity* **29**, 375 (2016).
- [42] J. Kullig and J. Wiersig, Frobenius–Perron eigenstates in deformed microdisk cavities: non-Hermitian physics and asymmetric backscattering in ray dynamics, *New J. Phys.* **18**, 015005 (2016).
- [43] N. Mertig, J. Kullig, C. Löbner, A. Bäcker, and R. Ketzmerick, Perturbation-free prediction of resonance-assisted tunneling in mixed regular-chaotic systems, [arXiv:1607.06477 \[nlin.CD\]](https://arxiv.org/abs/1607.06477) (2016).
- [44] P. Schlagheck, A. Mouchet, and D. Ullmo, Resonance-assisted tunneling in mixed regular-chaotic systems, in “Dynamical Tunneling: Theory and Experiment”, [2], chapter 8, 177.
- [45] G. D. Birkhoff, Proof of Poincaré’s geometric theorem, *Trans. Amer. Math. Soc.* **14**, 14 (1913).
- [46] C. Löbner, S. Löck, A. Bäcker, and R. Ketzmerick, Integrable approximation of regular islands: The iterative canonical transformation method, *Phys. Rev. E* **88**, 062901 (2013).
- [47] J. Kullig, C. Löbner, N. Mertig, A. Bäcker, and R. Ketzmerick, Integrable approximation of regular regions with a nonlinear resonance chain, *Phys. Rev. E* **90**, 052906 (2014).
- [48] J. Le Deunff, A. Mouchet, and P. Schlagheck, Semiclassical description of resonance-assisted tunneling in one-dimensional integrable models, *Phys. Rev. E* **88**, 042927 (2013).
- [49] B. V. Chirikov, A universal instability of many-dimensional oscillator systems, *Phys. Rep.* **52**, 263 (1979).
- [50] A. M. Ozorio de Almeida, Tunneling and the semiclassical spectrum for an isolated classical resonance, *J. Phys. Chem.* **88**, 6139 (1984).
- [51] M. V. Berry and K. E. Mount, Semiclassical approximations in wave mechanics, *Rep. Prog. Phys.* **35**, 315 (1972).
- [52] S. Creagh, Tunnelling in multidimensional systems, *J. Phys. A* **27**, 4969 (1994).
- [53] J. M. Greene and I. C. Percival, Hamiltonian maps in the complex plane, *Physica D* **3**, 530 (1981).
- [54] I. C. Percival, Chaotic boundary of a Hamiltonian map, *Physica D* **6**, 67 (1982).